Available online at www.sciencedirect.com
ScienceDirect
C. R. Physique 9 (2008) 517–523
COMPTES RENDUS PHYSIQUE
http://france.elsevier.com/direct/COMREN/

Synchrotron x-rays and condensed matter/Rayonnement X synchrotron et matière condensée

# Does band mapping find its limits in the soft X-ray range?

Federica Venturini *, Nicholas B. Brookes

*ESRF, European Synchrotron Radiation Facility, BP 220, 38043 Grenoble, France*

Available online 7 November 2007

**Abstract**

The (001) surface of Silver (Ag) has been chosen as a simple and well known system for investigating the band mapping potentialities of angle-resolved photoemission spectroscopy in the soft X-ray energy range. In order to determine the intrinsic limits of this technique, the valence band of Ag has been measured both as a function of the measuring temperature and of the incoming photon energy and the issue of phonon-assisted non-direct transitions is addressed. ***To cite this article: F. Venturini, N.B. Brookes, C. R. Physique 9 (2008).***


**Résumé**

**La détermination de la structure de bandes trouve-t-elle ses limites dans le domaine des rayons X mous ?** Nous avons choisi la surface (001) de l'Argent (Ag), qui est un système simple et bien connu, pour étudier le potentiel, en matière d'étude de la structure de bandes, de la spectroscopie de photoémission résolue en angle dans le domaine d'énergie des rayons X mous. Pour déterminer les limites intrinsèques de cette technique, nous avons mesuré la bande de valence de l'argent en fonction de la température et de l'énergie du photon incident. Nous discutons aussi la question des transitions indirectes assistées par phonon. ***Pour citer cet article : F. Venturini, N.B. Brookes, C. R. Physique 9 (2008).***


*Keywords:* Band mapping; Silver surface; Photoemission spectroscopy

*Mots-clés :* Étude de la structure de bandes ; Surface d'argent ; Spectroscopie de photoémission

## 1. Introduction

Angle-resolved photoemission spectroscopy (ARPES) [1,2] is well known for being a powerful and direct tool for probing the occupied electronic states of solids and, recently, great improvements have been made in both the energy and the angular resolution that can be obtained with the technique [3,4]. Such an advancement, however, has not been extended to three dimensional systems, the major limitation being that, due to the lack of translational symmetry along the surface normal, the initial state wave vector along this direction, $k_{\mathrm{perp}}$, is not conserved. Within the direct transition model, that describes the photoemission process as a succession of three independent events, namely the optical excitation of the electrons within the crystal, their propagation to the surface and their escape into the vacuum, the non-conservation of $k_{\mathrm{perp}}$ is overcome by assuming a free-electron-like final state. Nevertheless, such

* Corresponding author.
*E-mail addresses:* venturin@esrf.fr (F. Venturini), brookes@esrf.fr (N.B. Brookes).

1631-0705/$ – see front matter 
doi:10.1016/j.crhy.2007.07.012

an approximation must be considered with care, as it is questionable for low excitation energies, especially so in the case of strongly correlated systems. For these, the availability of photons belonging to the soft X-ray energy range ($400\ \text{eV} \leqslant h\nu \leqslant 1500\ \text{eV}$) guarantees, upon excitation, the formation of a photoelectron final state that is effectively decoupled from the remaining system. Added to this, if the photon energy is increased to the soft X-ray range, the angle needed to cover a Brillouin zone becomes considerably smaller if compared to the low energy application of the same technique. As a consequence, the corresponding $k$-space curvature is negligible when compared to the zone size and the energy dispersion along any high symmetry direction can be measured directly. Also, for systems whose electronic structure differs markedly from surface to bulk [5], higher incoming energies ensure more bulk representative results [6,7] due to the increase of the inelastic mean free path. However, several issues hamper an unconditional use of this technique in the soft X-ray range. First of all, the measurements can suffer from momentum averaging effects, brought on by the participation of the phonons in the photoemission process, that prevent accurate band mapping experiments. A different, but equally important issue, is the role of the photon momentum, $k_{h\nu} = 2\pi/\lambda$, that can no longer be neglected as is justifiably done in the low photon energy regime. To give an example, in the particular case of Ag, whose lattice constant and radius of the Brillouin zone are respectively $a = 4.09\ \text{Å}^{-1}$ and $2\pi/a = 1.54\ \text{Å}^{-1}$, at $h\nu = 21.2$ eV the photon momentum is only 0.5% of the zone radius whereas for $h\nu = 1487$ eV it is nearly 50%. However, as will be shown in the following, despite the relatively high incoming energies, a careful choice of the experimental geometry can minimise the effect of $k_{h\nu}$. From a more technical point of view, due to the strong decrease of the photoionisation cross-section with increasing photon energy [8], high energy resolution measurements are very demanding and the development of the technique has represented a major challenge. Last but not least, high angular resolution is also required since the momentum resolution not only depends on the angular resolution but also on the square root of the kinetic energy. Nowadays, thanks to the availability of dedicated photoemission beamlines and performing electron analysers that ensure a high photon flux at the sample, a high energy resolution of the monochromatised light, and a high resolution performance of the electron analyser, measuring soft X-ray angle-resolved photoemission spectra with relatively high energy and momentum resolution is possible [6,7,9–14].

In this article we discuss the potential of soft X-ray angle-resolved photoemission spectroscopy. In order to investigate the possibility of performing accurate band mapping experiments in the soft X-ray energy range, Silver (Ag) has been chosen as a well known metal whose electronic band structure has been extensively studied both from a theoretical [15–21] and an experimental point of view [22–30]. Measurements along one high symmetry direction have been recorded for different values of both the incoming photon energy and the temperature. The possibility of performing accurate band mapping experiments within the soft X-ray range is clearly evidenced, although the temperature of the investigated system plays an important role in determining the appropriate temperature and photon energy combinations at which similar experiments can be performed.

## 2. The effect of phonon disorder

Numerous studies [31–36] have demonstrated that the simple direct transition model can indeed predict most of the structures observed in photoemission spectra obtained with $h\nu \leqslant 200$ eV. Although initially calculations based upon this approach were also found to qualitatively predict the spectral changes observed in the higher energy regime [37, 38], subsequent experimental studies indicated that at these energies a rather complete averaging out over reciprocal space occurs [39,40]. The observation of strong direct transition effects in the low and intermediate energy range, and the full zone averaging that takes place for $h\nu \approx 10^3$ eV, was first explained by Shevchik [41–43]. It appeared that thermal disorder destroys the conservation of the initial state wave vector, $k$, during the photoemission process and that this phenomenon becomes extremely important for most materials at room temperature and/or X-ray photoemission incoming energies. In particular, two different contributions give rise to the photoemission spectrum: one originates from the $k$-conserving direct transitions, the other one from the so-called phonon-assisted non-direct transitions. The weaker selection rule imposed on $k$ in the latter contribution allows transitions from different regions of the Brillouin zone giving rise to density-of-states-like spectra. Within the simple model, the relative importance of the two different contributions is determined by the temperature dependent Debye–Waller factor, $W(T)$:

$$W(T) = \exp\left[-\frac{1}{3} \cdot \Delta k^2 \cdot U^2(T)\right] \tag{1}$$

where $\Delta k$ is the wave vector change associated with the scattering and $U^2(T)$ is the mean square displacement of the atoms within the solid. In a simple one-electron picture, angle-resolved photoemission spectroscopy can be seen as a diffraction process in which the incident beam is represented by an initial state given by a photon of momentum $k_{h\nu}$ and a bound valence electron state of momentum $k$, whereas the scattered beam is given by the final state of momentum $K$. Therefore the diffraction law describing elastic scattering by a crystal lattice also describes the direct transition requirement in photoemission spectroscopy through the identity:

$$\Delta k = K - (k + k_{h\nu}) = G \tag{2}$$

where $G$ is a reciprocal lattice vector. Very simply, this implies that the intensity of a direct transition peak is expected to exhibit a temperature dependence that is consistent with Eq. (1) as well as a photon energy dependence given by the change in $\Delta k = G$ with changing $h\nu$. It follows that the non-direct transitions become more significant at high temperatures and/or at high excitation energies. For room temperature photoemission studies direct transition processes should dominate in most metals at ultra-violet photoemission energies, whereas, due to the large value of $G$, the phonon-assisted processes are expected to take the lead in the X-ray photoemission regime.

The temperature dependence of the valence band spectra expected as a result of such phonon-induced transitions was experimentally observed for the first time in a low energy angle-resolved photoemission experiment performed on Cu [44]. For high incoming photon energies, the temperature dependence of the photoemission spectra suggested in [41–43] was first observed for tungsten, W [45,46]. In particular, the direct transition component of the photoemitted intensity was found to be consistent with a simple direct transition model based on constant matrix elements and a free-electron-like final state, in agreement with [37,38]. On the other hand, the non-direct transition component appeared to be similar to the density of states weighted by the appropriate matrix elements. In more recent investigations [13, 14,47] temperature and photon energy dependent angle-resolved photoemission spectra from Al have been analysed with a model that allows one to calculate the contributions to the photoemitted intensity for transitions in which $m$ phonons have been excited or absorbed, with $m = 0, 1, 2, \ldots$. The lattice vibrations are treated within the Debye model and larger vibrational amplitudes at the surface are taken into account. The results clearly show a decay of the direct transition peak with increasing temperature and photon energy that can be qualitatively understood in terms of Shevchik's model. Nevertheless, it is shown that the direct transition peaks also contain contributions from electrons that have been scattered by one or more phonons.

## 3. Experimental considerations

The experiments have been carried out at the ID08 soft X-ray beamline at the European Synchrotron Radiation Facility in Grenoble, France. The beamline is equipped with a Scienta SES-2002 electron analyser that is coupled to an ultra-high vacuum chamber. The first Brillouin zone of Ag is shown in the left panel of Fig. 1 where the different high symmetry points and directions are labelled with capital letters and symbols respectively.

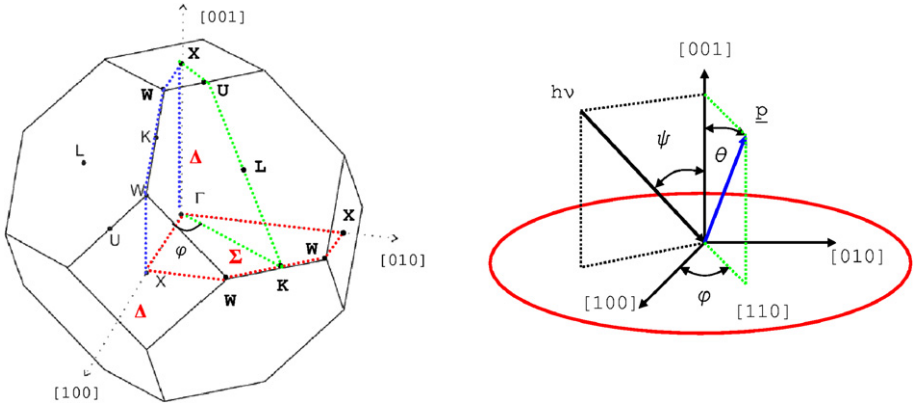


Fig. 1. Left: Brillouin zone of Ag with high symmetry points and directions. Right: schematic representation of the experimental geometry. The angle of incidence of the light with respect to the [001] direction is fixed and $\psi = 35°$. The photoelectron emission plane is normal to the plane containing the incident light and the normal to the surface. Different emission planes can be probed by varying the azimuthal angle, $\varphi$.

The (001) surface of a single crystal sample of Ag has been cleaned in situ by argon-ion bombardment and annealed at temperatures ranging between 450 and 550 °C in order to remove any surface damage given by the cleaning procedure. Several cleaning cycles are necessary to obtain an optimal surface. Throughout the measurements the base pressure in the main experimental chamber is kept below $10^{-10}$ mbar. The cleanliness of the surface is checked by monitoring the C and O 1s peaks with core level X-ray photoemission spectroscopy and both types of contaminations are absent for the whole length of the data acquisition. Low energy electron diffraction (LEED) is used to verify the good surface order and to specify the orientation of the sample. A continuous flow of liquid He allows for the sample cooling and the heating system consists of a spirally-wound filament positioned on the sample holder. The experimental geometry is sketched in the right panel of Fig. 1. The angle, $\psi$, between the incident light and the surface normal is fixed and equal to 35°. The sample holder allows for polar, $\Theta$, and azimuthal, $\varphi$, rotations as well as for the adjustment of the $\beta$ angle that defines the tilt of the sample's surface with respect to the entrance plane of the electron analyser. Polar rotations are performed about the axis that is perpendicular to the plane containing the direction of X-ray incidence and the surface normal, whereas azimuthal rotations are about the surface normal and the azimuth angle, $\varphi$, is measured with respect to the [100] crystallographic direction. The electron emission, defined by the $\vartheta$ angle measured with respect to the [001] direction, takes place in a plane that is perpendicular to the one defined by the incoming radiation and the surface normal. Therefore, referring to Fig. 1, when $\varphi = 45°$, the photon momentum has no component along the [110] crystallographic direction. The effect of the photon momentum along the $[\bar{1}10]$ direction is to 'kick' the photoelectron in a direction that is perpendicular to the probed high symmetry direction. This effect is corrected for during the initial alignment procedure that is used to determine the normal emission angle, $\Theta$. In order to take into account the photon momentum transferred along the [001] direction, the free-electron-like final state approximation is modified by simply adding a factor $k_{h\nu}\cos\psi = k_{h\nu}\cos 35°$ to the expression that is generally used in the low energy range:

$$K_{\text{perp}} = \sqrt{2m/\hbar^2(E_{\text{Kin}} + V_0)} + k_{h\nu}\cos\psi \tag{3}$$

By doing so, Eq. (3), that describes the variation with photon energy of the final state wave vector in the direction perpendicular to the surface, accurately follows the experimental determination of the high symmetry points along this direction.

## 4. Results and discussion

In order to investigate the limits of soft X-ray angle-resolved photoemission spectroscopy, data have been collected both as a function of the measuring temperature and of the incoming photon energy. If the inner potential is chosen as $V_0 = 10.5$ eV [16] then, according to Eq. (3), the values of $h\nu$ that correspond to three consecutive $X$ points along the [001] direction are $h\nu = 422$ eV, $h\nu = 698$ eV and $h\nu = 1040$ eV. The three equivalent high symmetry points are reached with $G = \frac{4\pi}{a}(0, 0, 3.5)$, $G = \frac{4\pi}{a}(0, 0, 4.5)$ and $G = \frac{4\pi}{a}(0, 0, 5.5)$ respectively. The azimuthal angle is kept constant and $\varphi = 45°$, thereby probing the $X$–$U$ high symmetry direction. The Debye temperature of Ag is known to be $\theta_{\text{D}} = 215$ K and for each value of $h\nu$ measurements have been taken for three different temperatures, $T = 20$ K, $T = 100$ K and $T = 215$ K. The Debye–Waller factors for each combination of $h\nu$ and $T$ are listed in Table 1, as obtained from Eq. (1). The data sets shown in the following are normalized to both the current at the sample and the acquisition time and the combined energy resolution of the beamline and the electron analyser are chosen to be similar for the different values of $h\nu$. Although in principle the chosen values of $h\nu$ probe three equivalent high symmetry points, when the photon energy increases the momentum resolution worsens and the mean free path of the outgoing photoelectrons increases. Hence the spectral features and the intensities of the data sets taken for different values of

Table 1
Debye–Waller factors, $W(T)$, calculated for nine different combinations of $T$ and $h\nu$ according to Eq. (1)

| | $h\nu = 422$ eV | $h\nu = 698$ eV | $h\nu = 1040$ eV |
|---|---|---|---|
| $T = 20$ K | 0.935 | 0.895 | 0.847 |
| $T = 100$ K | 0.715 | 0.574 | 0.437 |
| $T = 215$ K | 0.488 | 0.305 | 0.170 |

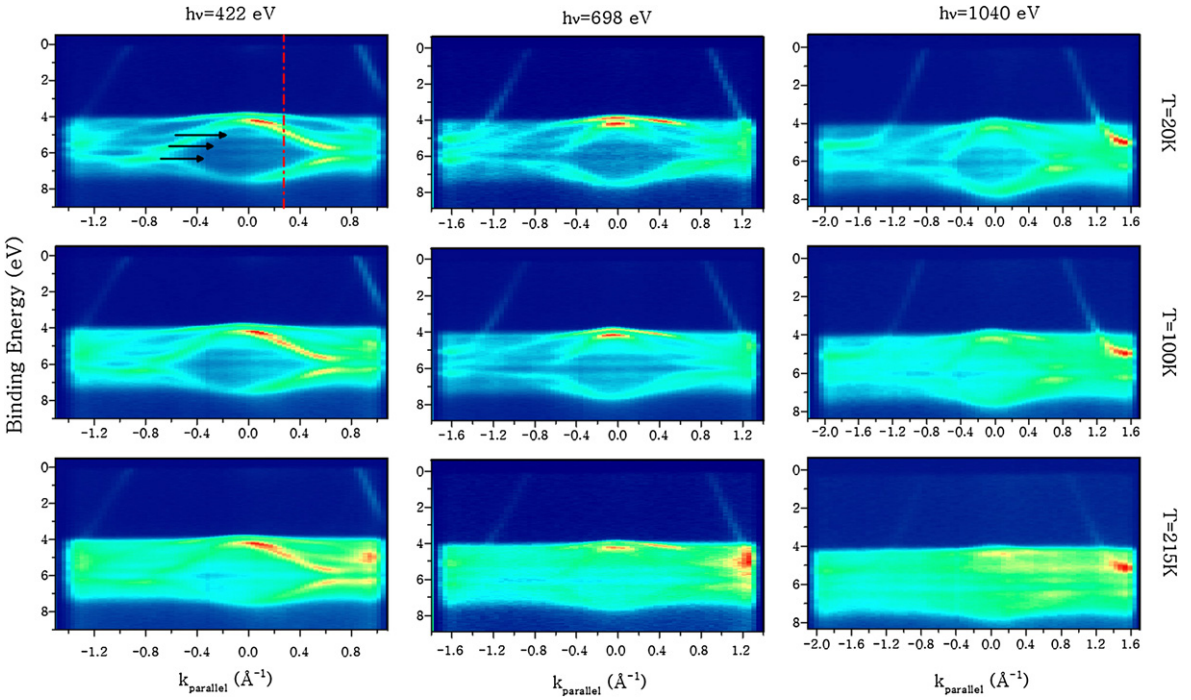


Fig. 2. $X$–$U$ high symmetry direction probed for nine different combinations of $T$ and $h\nu$. From left to right: $h\nu = 422$ eV, $h\nu = 698$ eV and $h\nu = 1040$ eV. From top to bottom: $T = 20$ K, $T = 100$ K and $T = 215$ K. $E_F = 0$ eV. The arrows in the upper left panel show the non-direct transitions, located approximately between 5 and 6.5 eV binding energy. The dashed line at $k_{par} \approx 0.25$ Å$^{-1}$ indicates the location in $k$-space of the energy distribution curves plotted in Fig. 3.

$h\nu$ at a given temperature cannot be directly compared. All the spectral variations observed with both temperature and photon energy are completely reversible and reproducible.

Fig. 2 shows the temperature dependence of the angle-resolved data for $h\nu = 422$ eV, $h\nu = 698$ eV and $h\nu = 1040$ eV from left to right. The zone boundary along the $X$–$U$ direction is found at $k_{par} \approx 0.51$ Å$^{-1}$. Along this direction $k_{par}$ varies from $X$ to $U = K$, and then further towards the $\Gamma$ point belonging to the next zone. This is unambigously observed, as the $s - p$ band belonging to the neighbouring Brillouin zone is seen crossing the Fermi level at $k_{par} \approx \pm 0.9$ Å$^{-1}$. Clearly, the nine measurements are qualitatively in agreement with Shevchik's model [41–43]. For $h\nu = 422$ eV the measured spectra can be compared with the band structure calculations discussed in [21]. In particular, the results obtained for $h\nu = 422$ eV and $T = 20$ K show a strong direct transition behaviour. Nevertheless, despite the low values of $h\nu$ and $T$, three features of constant binding energy are seen crossing the zone centre between approximately 5 and 6.5 eV. These features, that have also been observed in the low energy results presented in [25], mark the existence of non-$k$-conserving transitions originating from initial states in regions of $k$-space that are not directly probed by our experimental geometry. However, for $h\nu = 422$ eV and $T = 215$ K a straightforward comparison with the known band structure becomes difficult, as the underlying intensity of the non-direct contributions increases.

For a given value of $k_{par}$, namely $k_{par} = 0.25$ Å$^{-1}$, Fig. 3 shows the energy distribution curves as a function of temperature, for both $h\nu = 422$ eV and $h\nu = 1040$ eV. As in Fig. 2, the existence of non-$k$-conserving transitions is clearly observed for both values of $h\nu$ between 5 and 6.5 eV binding energy although, given the location in $k$-space that is investigated, the feature positioned at approximately 5 eV is hidden by the more intense direct transitions. For a given photon energy, as the temperature is increased the intensity of these features also increases. However, this is done at the expenses of the intensity of the direct transitions, whose spectral representations are labelled as a, b, c and d, respectively. A similar effect can be observed for a given temperature as a function of the photon energy although, as previously mentioned, given the increase of the inelastic mean free path with increasing photon energy, the intensity of features measured at the same temperature but for different values of $h\nu$ should not be directly

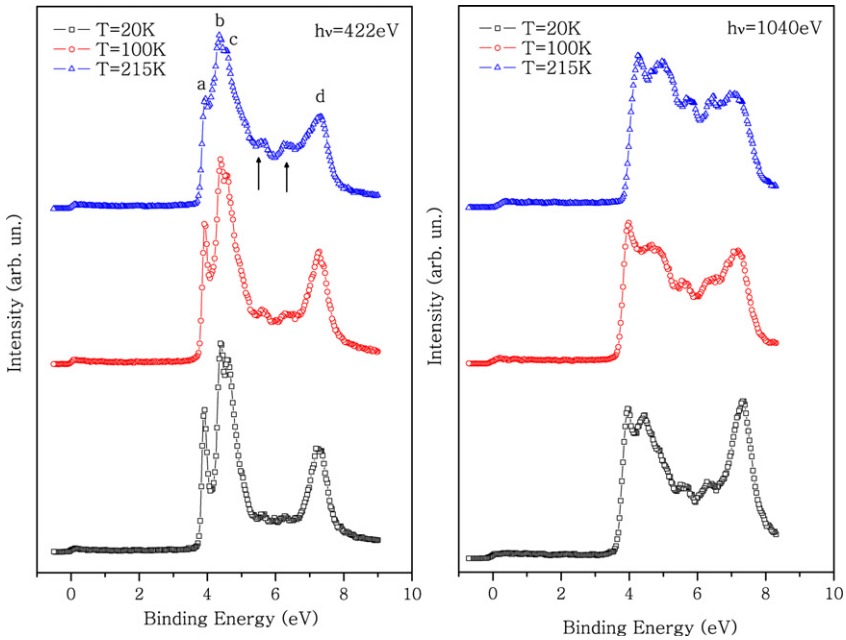


Fig. 3. Energy distribution curves measured for $k_{\mathrm{par}} = 0.25$ Å$^{-1}$. Left panel: $h\nu = 422$ eV. Right panel: $h\nu = 1040$ eV. From bottom to top: $T = 20$ K, $T = 100$ K and $T = 215$ K. The direct transitions are marked as a, b, c and d. The visible non-direct transitions are evidenced by the arrows.

compared. Consistently with the model, as the temperature and the photon energy are increased, the phonon-assisted transitions also increase. In the particular case of $h\nu = 1040$ eV, at $T = 20$ K the direct transition features can still be distinguished but strong modifications of the line shape and of the relative intensities are already visible, whereas for $h\nu = 1040$ eV and $T = 215$ K the data have lost most of their structure and band like features are barely visible. These results indicate that, in the particular case of Ag ($\theta_{\mathrm{D}} = 215$ K), the transition from a band-like to a density of states-like behaviour, called the XPS limit, has already been reached for $h\nu = 1040$ eV and $T = 215$ K.

## 5. Conclusions

The investigation performed on the (001) surface of Ag addresses several questions regarding the application of angle-resolved photoemission spectroscopy in the soft X-ray energy range, such as the feasibility of accurate band mapping experiments and the role of the photon momentum. Despite the accuracy of the results obtained at low temperature ($T = 20$ K) for both $h\nu = 422$ eV and $h\nu = 698$ eV, the temperature and photon energy dependent study clearly shows the onset, in the high $T$ and/or in the high photon energy range, of the non-direct transitions caused by the breakdown of the $k$-conservation laws. Our results show that the contribution of the non-direct transitions to the photoemitted intensity is indeed controlled by a delicate balance between $h\nu$ and $T$. Finally, if the experimental geometry is chosen with care, the effect of the photon momentum can be restricted to the direction perpendicular to the investigated surface, therefore allowing us to accurately take it into account.

To conclude, a constructive development of an experimental technique comes with the awareness of its limits and precise soft X-ray band mapping is possible if restricted to a rather small range of temperatures and photon energies. In particular, for a given value of the Debye temperature, $\theta_{\mathrm{D}}$, the higher the incoming photon energy, the lower the temperature required for an accurate determination of the band structure. If compared to the low energy application of the same technique, the increased energy of the incoming photons allows for more bulk sensitive investigations. This is particularly important for the comprehension of the electronic structure of many highly correlated systems of interest today, such as high $T_c$ superconductors and Ce compounds for example, whose surface electronic structure differs considerably from the bulk one. In order to further understand the limits of soft X-ray band mapping, we hope that these results will stimulate future theoretical calculations.

## References


[1] S. Hüfner, J. Phys. Soc. Jpn. 74 (2003) 34.
[2] F.J. Himpsel, Adv. Phys. 32 (2005) 1.
[3] T. Kiss, et al., Phys. Rev. Lett. 94 (2005) 057001.
[4] Y. Baer, M.G. Garnier, D. Purdie, P. Segovia, M. Hengsberger, J. Electron Spectrosc. Relat. Phenom. 114 (2001) 257.
[5] L. Duò, Surf. Sci. Rep. 32 (1998) 235.
[6] T. Claesson, M. Mansson, C. Dallera, F. Venturini, C. De Nadaï, N.B. Brookes, O. Tjernberg, Phys. Rev. Lett. 93 (2004) 136402.
[7] F. Venturini, J.C. Cezar, C. De Nadaï, P.C. Canfield, N.B. Brookes, J. Phys.: Condens. Matter 18 (2006) 9221–9229.
[8] J.J. Yeh, I. Lindau, At. Data Nucl. Data Tables 32 (1985) 1.
[9] S. Suga, S. Sekiyama, J. Electron Spectrosc. Relat. Phenom. 124 (2002) 81–97.
[10] S. Suga, et al., Phys. Rev. B 70 (2004) 155106.
[11] A. Sekiyama, et al., Phys. Rev. B 70 (2004) 060506(R).
[12] A. Sekiyama, S. Suga, J. Electron Spectrosc. Relat. Phenom. 137–40 (2004) 681.
[13] C. Sondergaard, P. Hofmann, C. Schultz, M.S. Moreno, J.E. Gayone, G. Zampieri, S. Lizzit, A. Baraldi, J. Phys. Rev. B 63 (2001) 233102.
[14] P. Hofmann, C. Sondergaard, S. Agergaard, S.V. Hoffmann, J.E. Gayone, G. Zampieri, S. Lizzit, A. Baraldi, J. Phys. Rev. B 66 (2002) 245422.
[15] E.C. Snow, Phys. Rev. 172 (1968) 708.
[16] N.E. Christensen, Phys. Status Solidi B 54 (1972) 551–563.
[17] N.V. Smith, Phys. Rev. B 9 (1974) 1365–1376.
[18] O. Jepsen, D. Glötzel, A.R. Mackintosh, Phys. Rev. B 23 (1981) 2684–2696.
[19] A.H. MacDonald, J.M. Daams, S.H. Vosko, D.D. Koelling, Phys. Rev. B 25 (1982) 713–725.
[20] R.L. Benbow, N.V. Smith, Phys. Rev. B 27 (1983) 3144–3151.
[21] H. Eckardt, L. Fritsche, J. Noffke, J. Phys. F: Met. Phys. 14 (1984) 97–112.
[22] H. Becker, E. Dietz, U. Gerhardt, H. Angermüller, Phys. Rev. B 12 (1975) 2084–2096.
[23] G.V. Hansson, S.A. Flodström, Phys. Rev. B 17 (1978) 473–483.
[24] P.S. Wehner, R.S. Williams, D. Kevan, D. Denly, D.A. Shirley, Phys. Rev. B 19 (1979) 6164–6171.
[25] R. Courths, V. Bachelier, S. Hüfner, Solid State Commun. 38 (1981) 887–889.
[26] H.A. Padmore, C. Norris, G.C. Smith, C.G. Larsson, D. Norman, J. Phys. C: Solid State Phys. 15 (1982) L155–L158.
[27] R. Courths, H. Wern, U. Hau, B. Cord, V. Bachelier, S. Hüfner, J. Phys. F: Met. Phys. 14 (1984) 1559–1572.
[28] J.G. Nelson, S. Kim, W.J. Gignac, R.S. Williams, J.G. Tobin, S.W. Robey, D.A. Shirley, Phys. Rev. B 32 (1985) 3465–3471.
[29] S.C. Wu, C.K.C. Lok, J. Sokolov, J. Quinn, Y.S. Li, D. Tian, F. Jona, J. Phys.: Condens. Matter 1 (1998) 4795–4804.
[30] U. König, P. Weinberger, J. Redinger, H. Erschbaumer, A.J. Freeman, Phys. Rev. B 39 (1989) 7492–7499.
[31] N.V. Smith, Phys. Rev. Lett. 23 (1969) 1452.
[32] N.V. Smith, Phys. Rev. B 3 (1971) 1862.
[33] J. Stöhr, G. Apai, P.S. Wehner, F.R. McFeely, R.S. Williams, D.A. Shirley, Phys. Rev. B 14 (1976) 5144–5155.
[34] J. Stöhr, P.S. Wehner, R.S. Williams, G. Apai, D.A. Shirley, Phys. Rev. B 17 (1978) 587–590.
[35] P. Thiry, D. Chandesris, J. Lecante, C. Guillot, R. Pinchaux, Y. Petroff, Phys. Rev. Lett. 43 (1979) 82–85.
[36] Z. Hussain, S. Kono, L.G. Petersson, C.S. Fadley, L.F. Wagner, Phys. Rev. B 23 (1981) 724–737.
[37] R.J. Baird, L.F. Wagner, C.S. Fadley, Phys. Rev. Lett. 37 (1976) 111–114.
[38] L.F. Wagner, Z. Hussain, C.S. Fadley, R.J. Baird, Solid State Commun. 21 (1977) 453–457.
[39] Z. Hussain, N.F.T. Hall, L.F. Wagner, S.P. Kowalczyk, C.S. Fadley, K.A. Thompson, R.L. Dodd, Solid State Commun. 11 (1978) 907–911.
[40] O.B. Dabbousi, P.S. Wehner, D.A. Shirley, Solid State Commun. 28 (1978) 227–231.
[41] N.J. Shevchik, Phys. Rev. B 16 (1977) 3428–3442.
[42] N.J. Shevchik, J. Phys. C: Solid State Phys. 10 (1977) L555–L557.
[43] N.J. Shevchik, Phys. Rev. B 20 (1979) 3020–3029.
[44] R.S. Williams, P.S. Wehner, J. Stöhr, D.A. Shirley, Phys. Rev. B 22 (1977) 3750–3766.
[45] Z. Hussain, C.S. Fadley, S. Kono, L.F. Wagner, Phys. Rev. B 22 (1980) 3750–3766.
[46] Z. Hussain, S. Kono, R.E. Connelly, C.S. Fadley, Phys. Rev. Lett. 44 (1980) 895–899.
[47] M.A.V. Alvarez, H. Ascolani, G. Zampieri, Phys. Rev. B 54 (1996) 14703–14712.